Additively Manufactured Heat Pipes

Payton Batliner, Alex Pagano, Natalie Walsh, John McHale, Jacob Rome, Payton Case, Xueyong (Kevin) Qu, Glenn Bean

Presented By

Payton Batliner & Alex Pagano

Thermal & Fluids Analysis Workshop
TFAWS 2022
September 6th-9th, 2022
Virtual Conference

Additively Manufactured Heat Pipes

Payton Batliner, Alex Pagano, Natalie Walsh, John McHale, Jacob Rome, Payton Case, Xueyong (Kevin) Qu, Glenn Bean

Thermal & Fluids Analysis Workshop
September 6-9, 2022

Additively Manufactured Heat Pipe (AMHP)Project

- Goal: design, print, and assess the functionality of an AMHP
  - *Use case: reduce unit temperatures and temperature gradients for similar production cost and schedule*
  - *Hypothesis: 3D printing will allow more optimized heat flow paths and fewer geometric constraints*
  - *Design integrates heat acquisition, heat transport, and heat rejection components into single fabrication*
  - *Removes interface resistances*

- Experiments were conducted comparing the temperature drop across an empty heat pipe to a methanol-filled heat pipe

- Filled heat pipe tests were compared to a numerical heat pipe modeling tool developed in Python by the Thermal Control Department (TCD)
  - *Target of 25% correlation error set for temperature drop predictions*

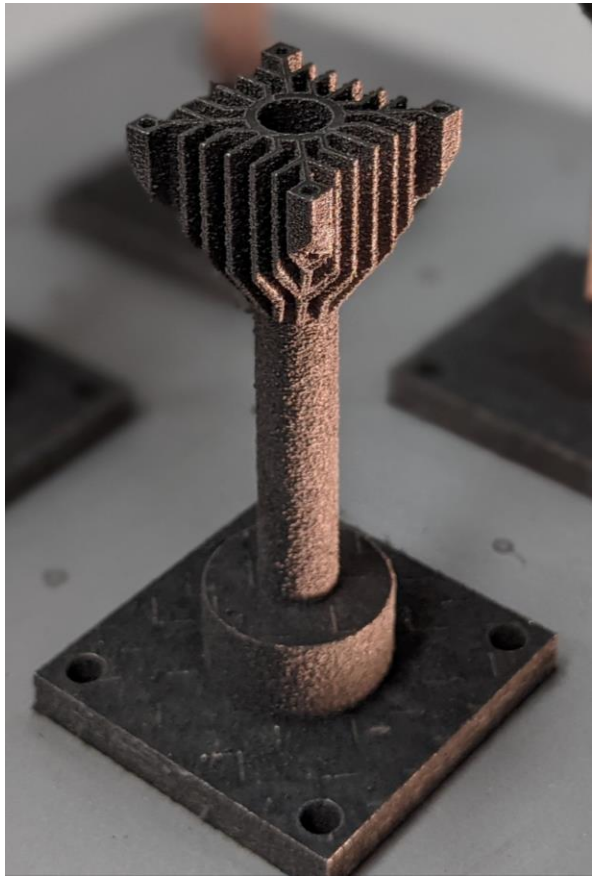

AMHP Test Article

AMHP Test Fixture Geometry

- AMHP test fixture geometry constrained by metal powder bed fusion (PBF) printing capabilities

- Overhangs
  - *(PBF) printing only allows a 35° overhang*
  - *Steeper overhangs require excessive support material*
    - Increased cost
    - Increased likelihood of printing failure
    - Very difficult to remove support material from inside the heat pipe
- Print orientation matters
  - *Traditional axially grooved design can be printed in vertical direction, but with path and size constraints*
    - Vertical prints only allow very minor curves in heat pipe path to be printed
    - Circular cross section with axial grooves is of interest for vertical prints
  - *Horizontal printing gives more freedom in terms of size and heat pipe path, but grooves cannot be printed around entire inner diameter of heat pipe*
    - Horizontal prints only allow certain heat pipe cross sections to be printed
    - Triangular cross section with wick on bottom is of interest for horizontal print
- Size requirements
  - *Small features can be lost in the print resolution (wick geometry, holes, etc.)*

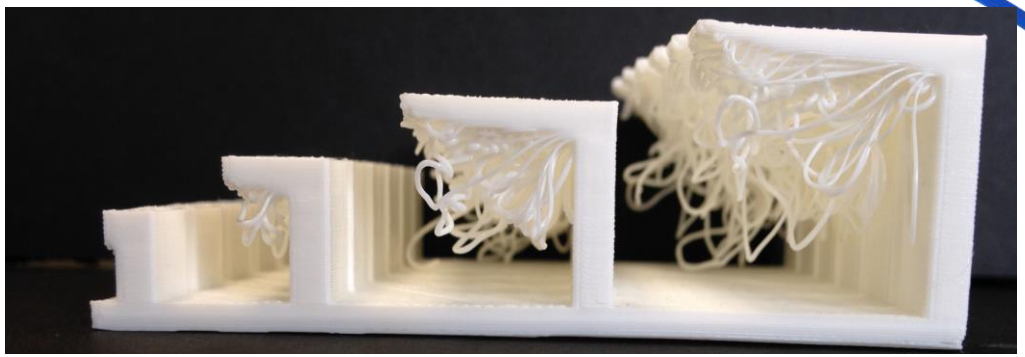

Vertical Printing

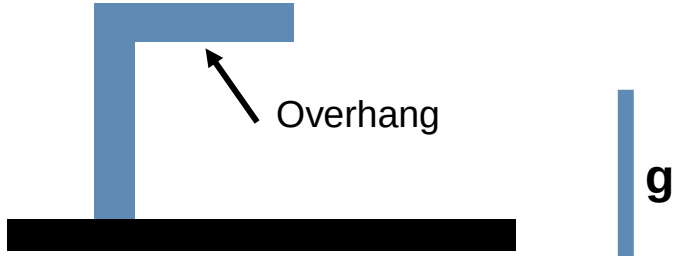

Horizontal Printing

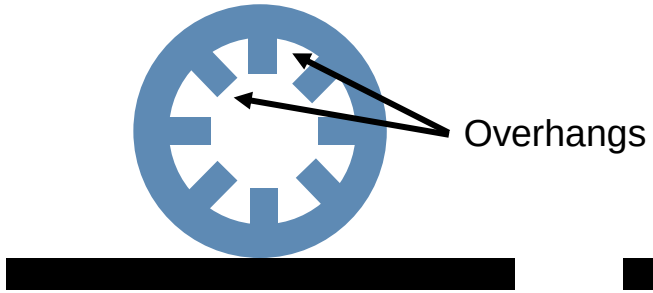

Circular Cross Section

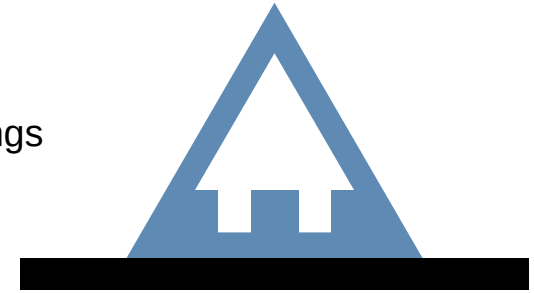

Triangular Cross Section

AMHP Test Article Design

- Initial objectives:
  - *Demonstrate failure-free printing of heat pipe geometry*
  - *Demonstrate heat pipe functionality*
  - *Explore a simple sealing approach*
- Vertical configuration to reduce risk of print failure
  - *Pipe had grooves around entire circumference (no wick overhang)*
  - *Heat rejection fin angle determined by maximum overhang able to be printed*
  - *Avoided curved paths – simplicity*
  - *Small features like wick and holes showed good resolution*
- SOLIDWORKS thermal simulation run to confirm adequate heat rejection capability of fan and finned heat sink
  - *Able to run test in air without chilled water loop*
- AMHP test article includes
  - *Flange with bolt holes to mount test article (tapped post-printing)*
  - *Bolt holes on finned section to attach fan (tapped post-printing)*

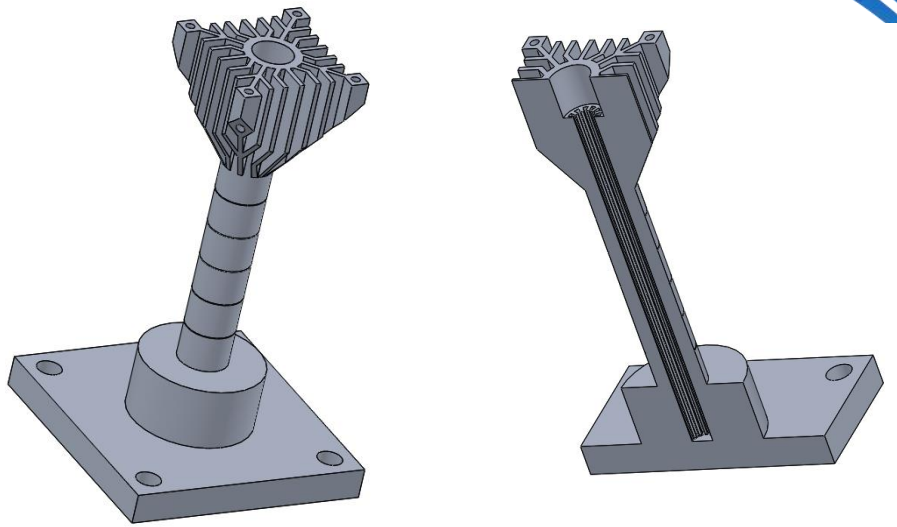

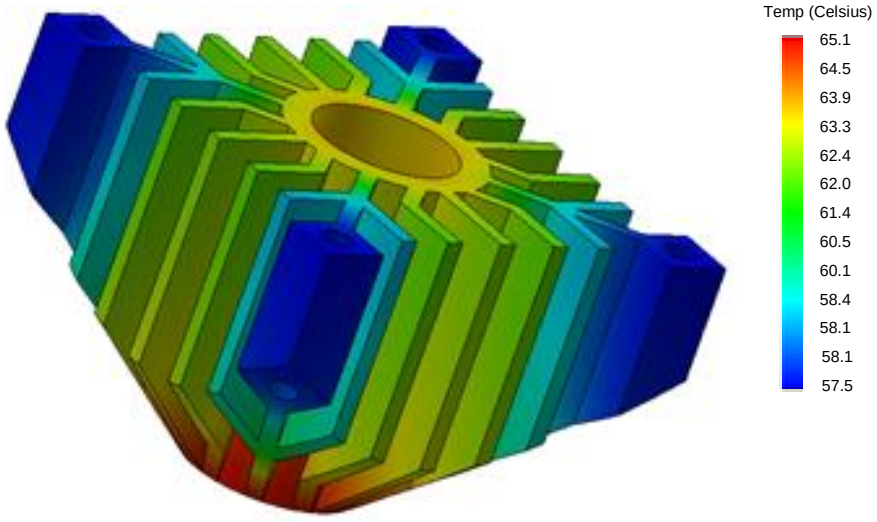

CAD of AMHP test fixture

Process Simulation and Residual Stress Assessment of Test Article

- Process simulation predicted a successful printing of heat pipe
  - *Analysis predicted no recoater blade crash and analysis was validated by the actual print*

- Max residual stress of 307 MPa predicted by structural assessment
  - *Material: AlSi10Mg*
    - Yield strength: 250 MPa
    - UTS around 310 to 325 MPa
  - *There is yielding, but no breakage*
  - *Elastoplastic stress at end of build*

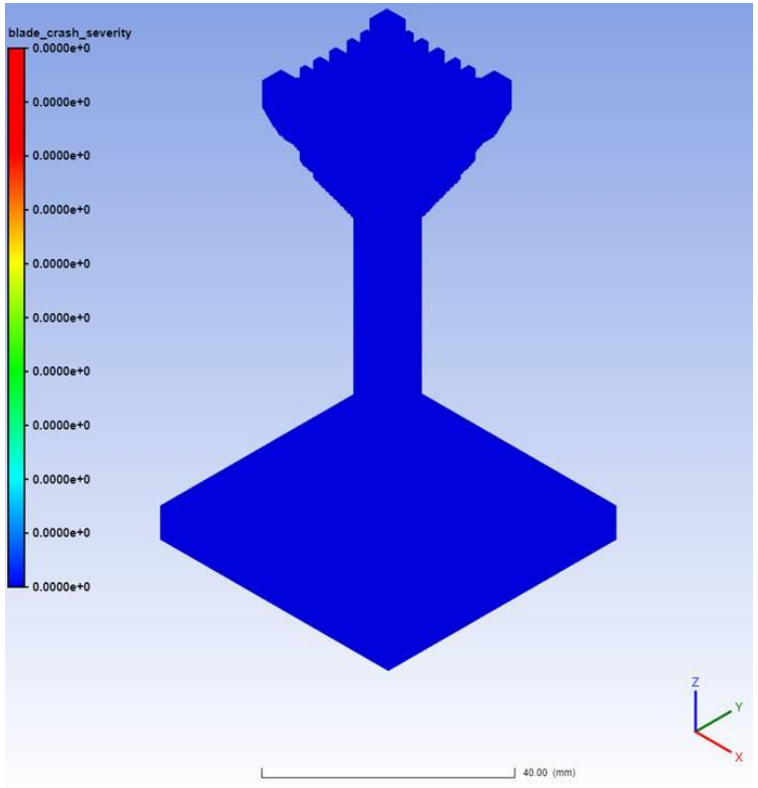

Process Simulation

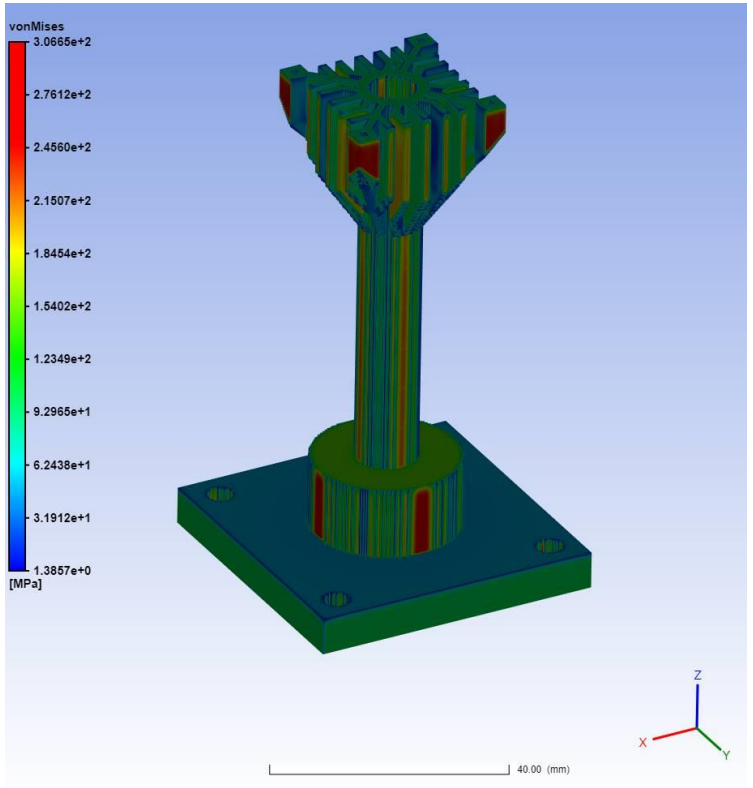

Residual Stress Analysis

Process simulations predicted a successful print and residual stress within material allowable limits

Prints

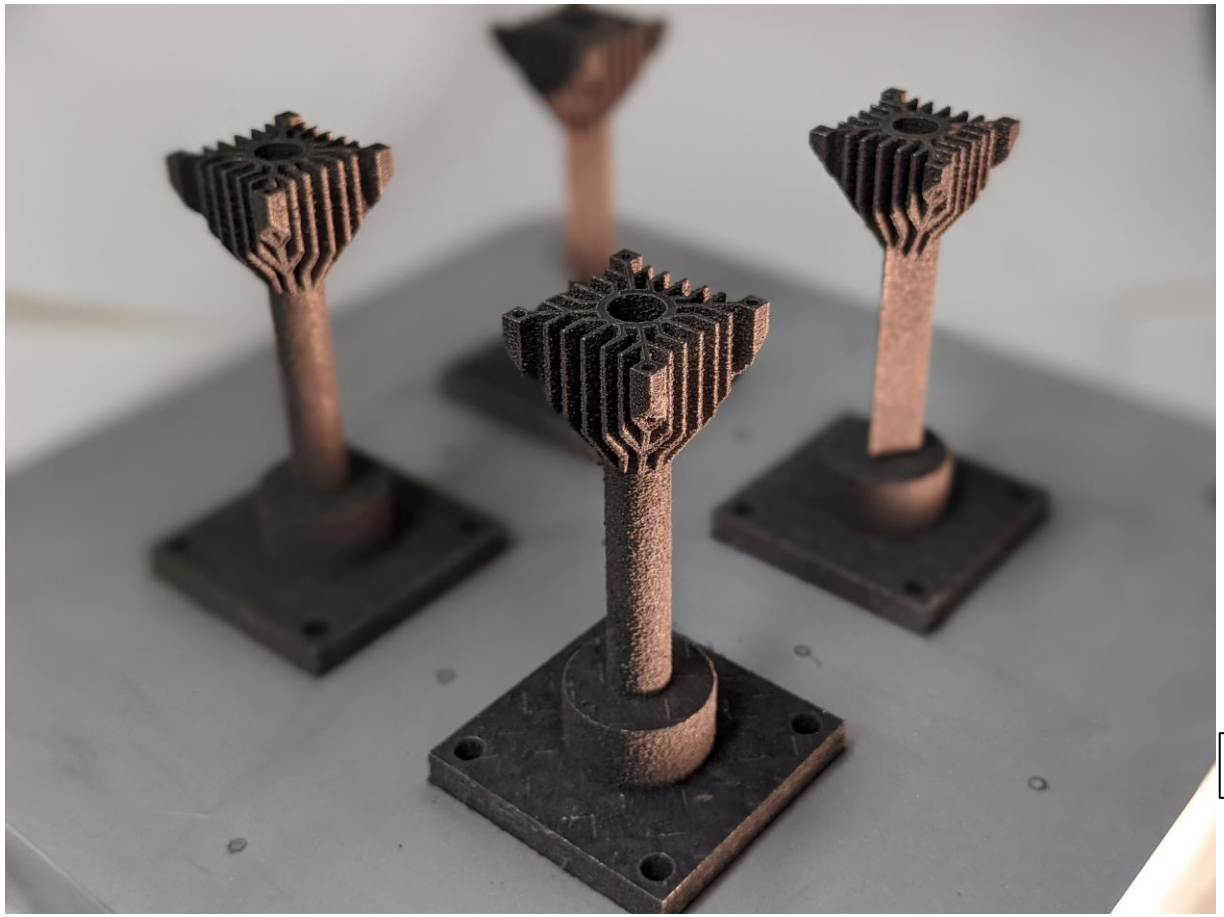

Prints on build plate

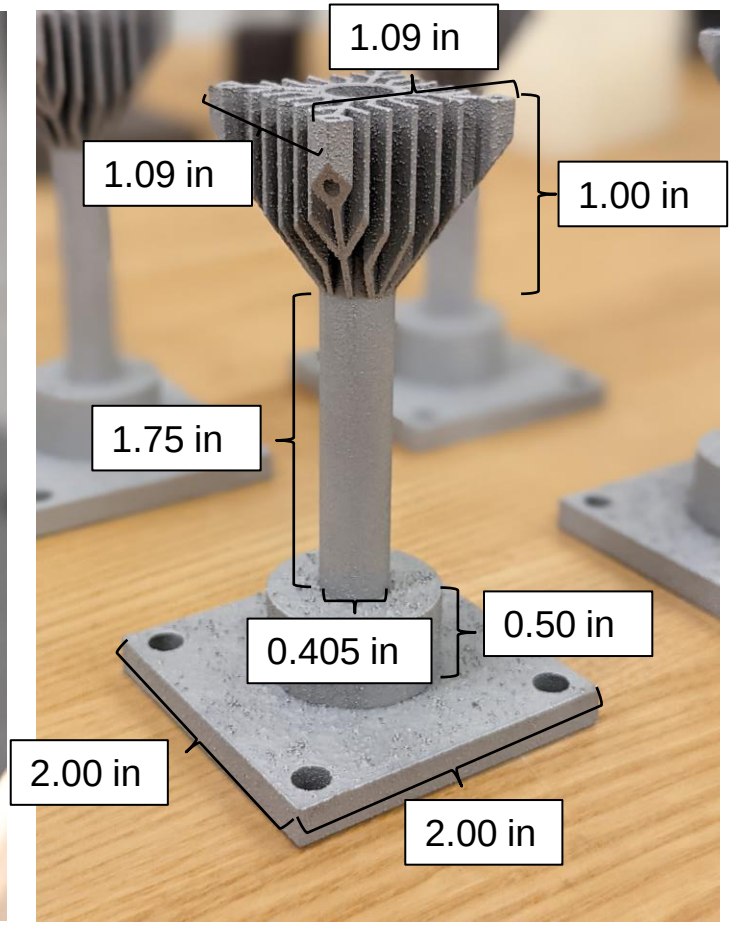

Prints after sand blasting

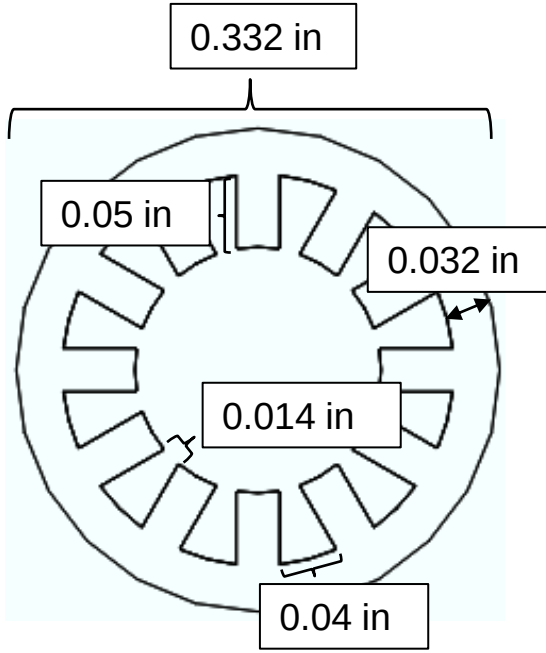

Wick cross-section

Printed using a laser powder bed fusion (LPBF) system and a 7000-series aluminum

Test Setup

- Setup bolted into G10 base plate to insulate the bottom flange
- Gap pad used to accommodate uneven surfaces between the heater and flange and prevent damage to the heater
- Kapton heater used to apply heat into base flange
  - *Constant voltage and measured current used to calculate power*
- 8 thermocouples applied along the length of the heat pipe
  - **TC8 applied beneath G10 base plate after filled data obtained in order to estimate heat flow losses*
- Fan placed on condenser section to provide heat rejection and reduce test temperature
- Swagelok fitting which is used to seal the heat pipe once it is filled
  - *Torr Seal used to seal Swagelok fitting to pipe to reduce leakage (NPT plug failed to seal)*
  - *Standoffs used to offset the fan to accommodate the Swagelok fitting*

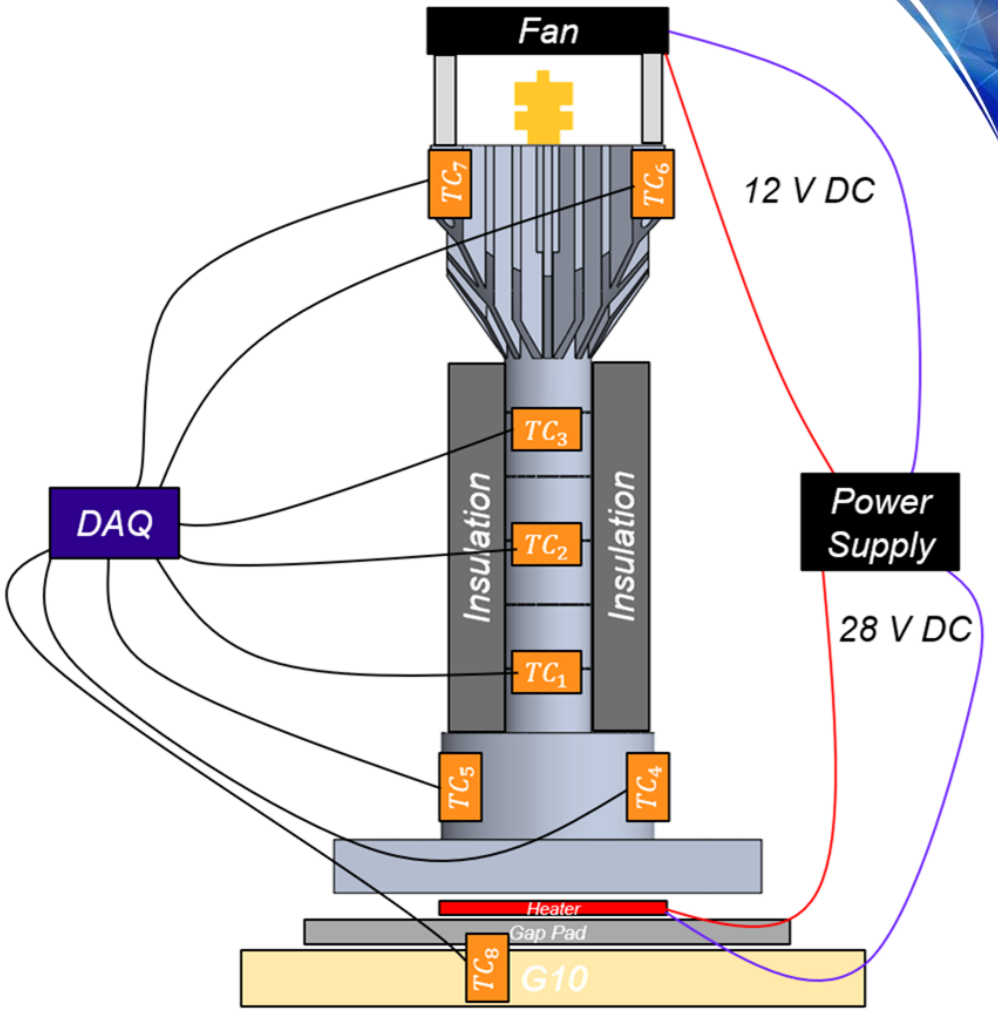

Test Procedure

- Place entire test article on balance, fill to 1 g
  - *Working fluid: methanol*
  - *Maximum fill volume: ~1.2 g*
- Fill / purge heat pipe using boil-off method
  - *Power on heater to 10 W, begin boiling fluid to purge non-condensables from heat pipe*
  - *As balance reading approaches desired charge mass, close pipe using Swagelok fitting*
- Attach fan to top of condenser section and power on fan
- Allow each thermocouple reading to reach steady state (~1 hour)
  - *Record ΔT from evaporator (TC 4&5) to condenser (TC 6&7)*
  - *Increment or decrement heater power and repeat*

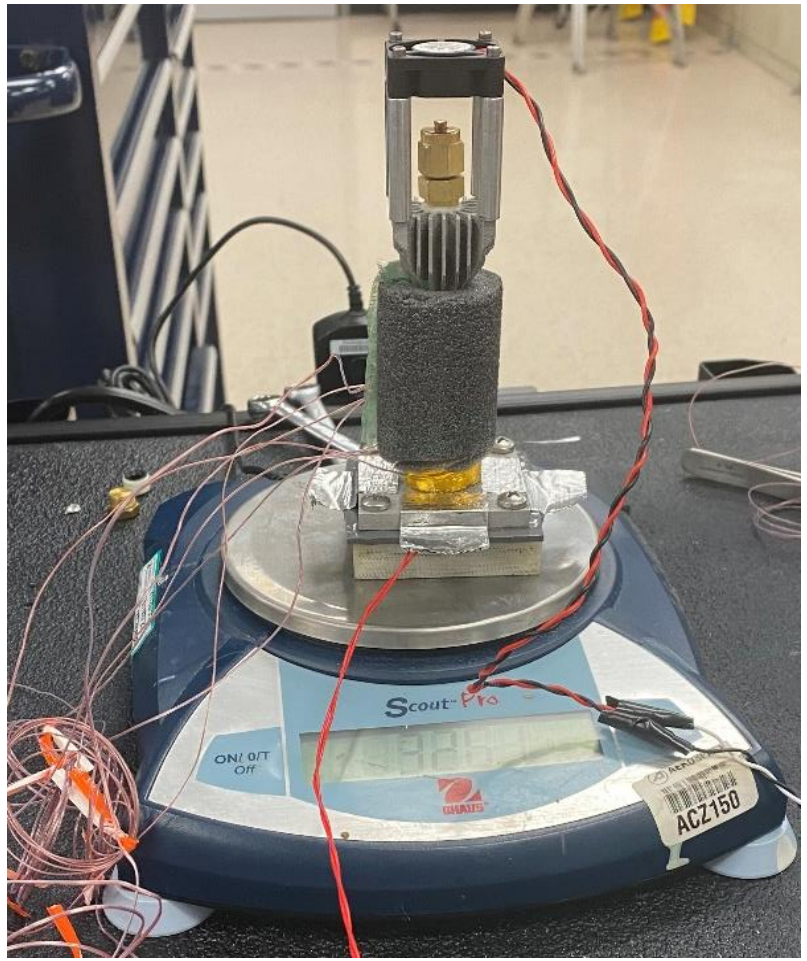

Test Results Overview

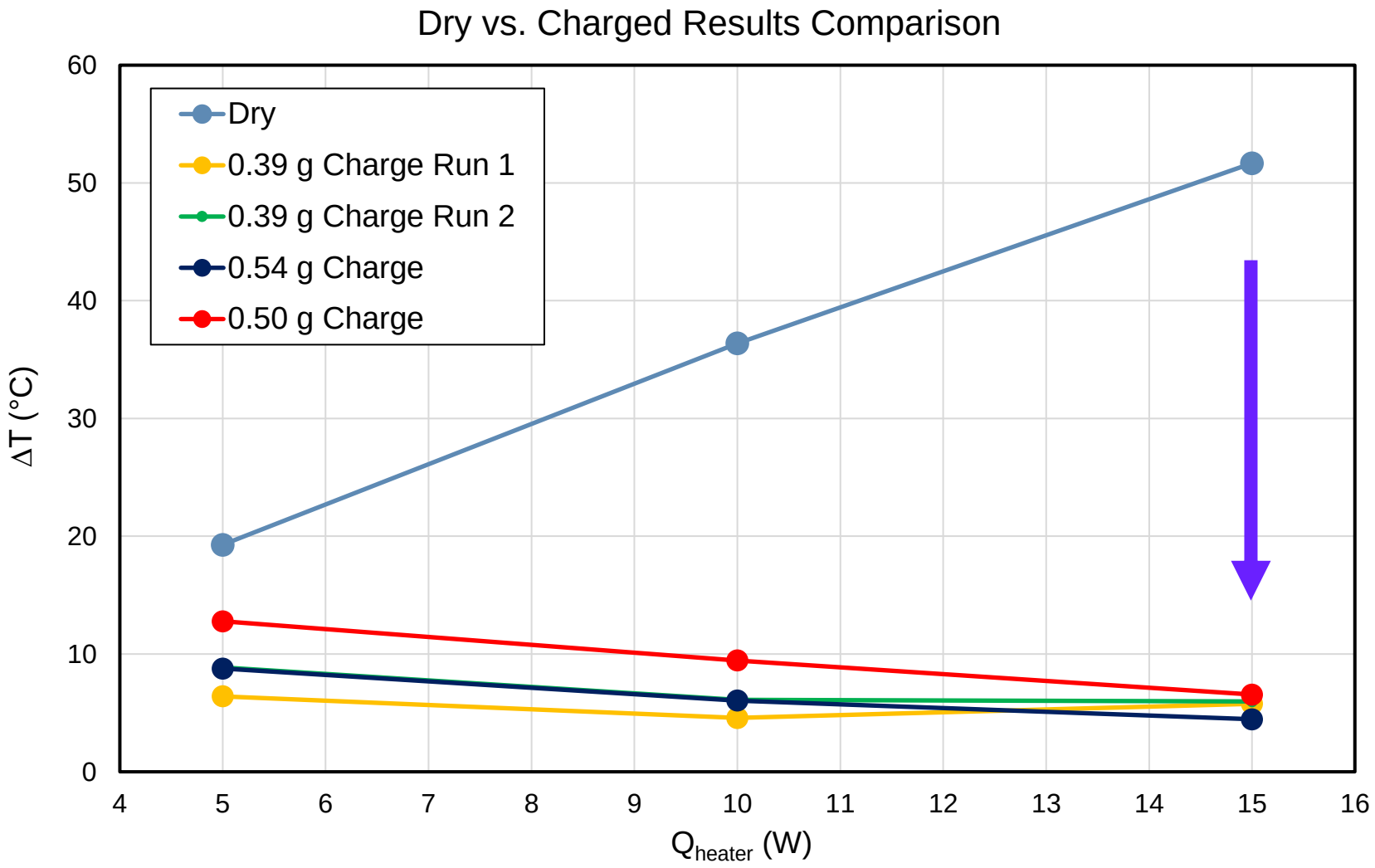

Q (W)	$\Delta T_{filled}/\Delta T_{dry}$
5	0.48
10	0.18
15	0.11

ΔT_{filled} averaged across four data sets

Significant average ΔT reduction seen across all four runs, particularly at higher heat input – heat pipe performance validated

Python Model Overview

- Model inputs: heat pipe cross-section geometry, fluid properties, desired heat input, charge mass, T_w etc.
- Model calculates the resistance between each node, incrementing the temperature to the following node based on the calculated resistance and heat input ($\Delta T = q * R$)
- R_{vap} due to hydrostatic & viscous vapor pressure drop (saturation temperature drop) and is typically negligible
- Condenser resistance (R_c) modeled based on Nusselt film condensation theory
- Evaporator resistance (R_e) corresponds to one of three different evaporator models (natural convection, partial nucleate boiling, full nucleate boiling) to capture delayed onset of boiling which depends on input power
- Model outputs total temperature drop and total pipe resistance for each evaporator model for a specified heat flow range and charge mass

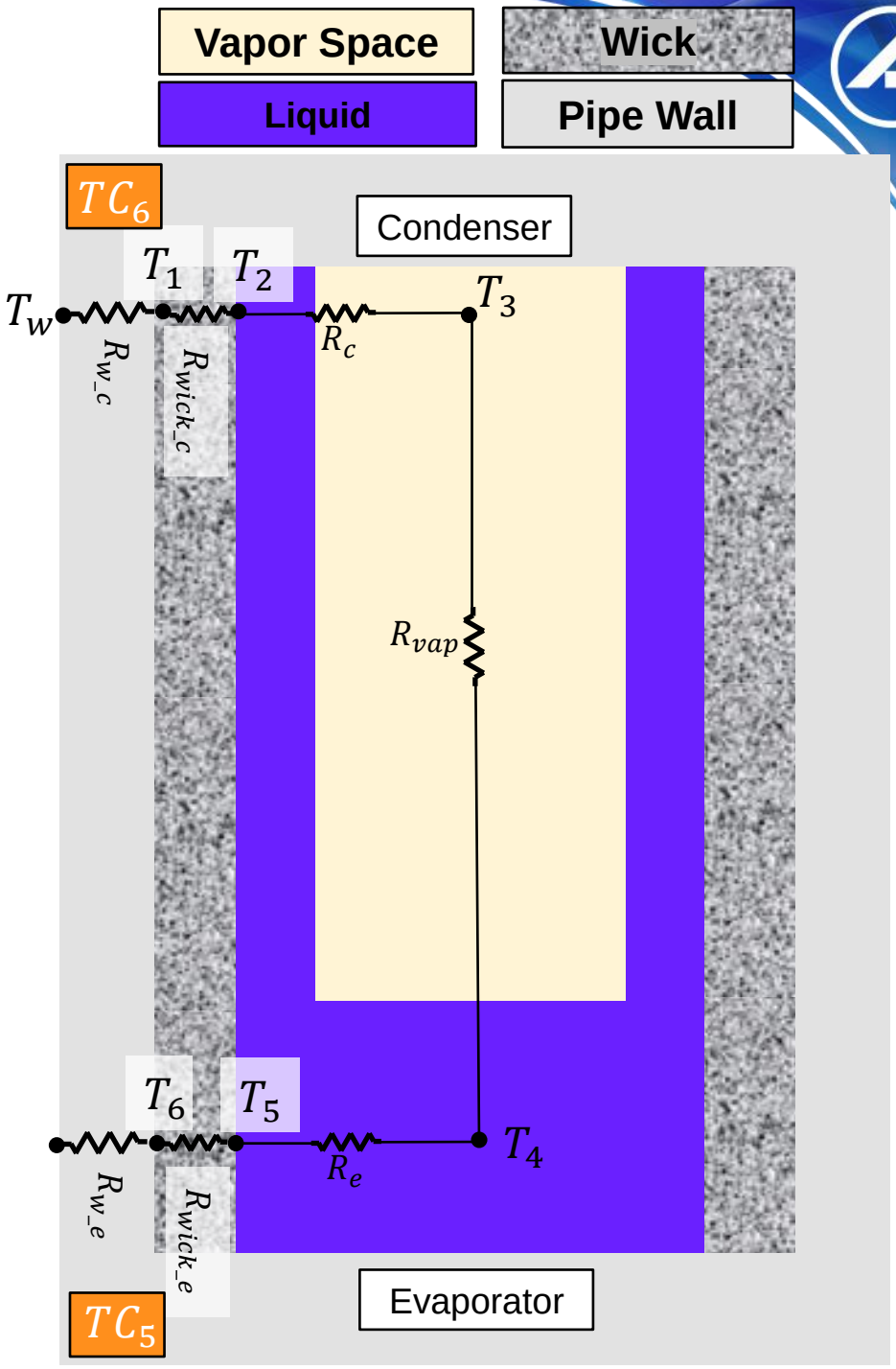

Python Model Sample Outputs

Temperature Drop & Total Resistance

Shaded region represents partial nucleate boiling regime – blue curve selected to represent partial nucleate boiling model.

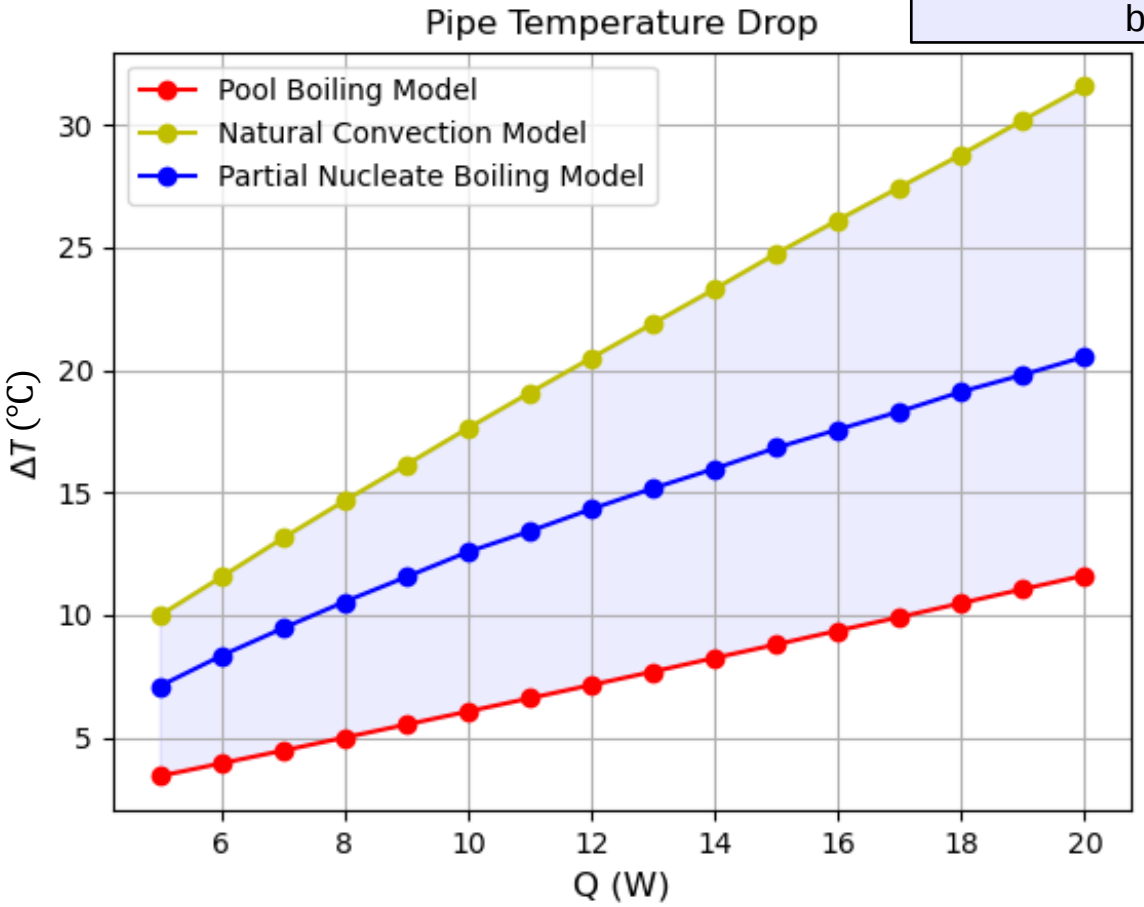

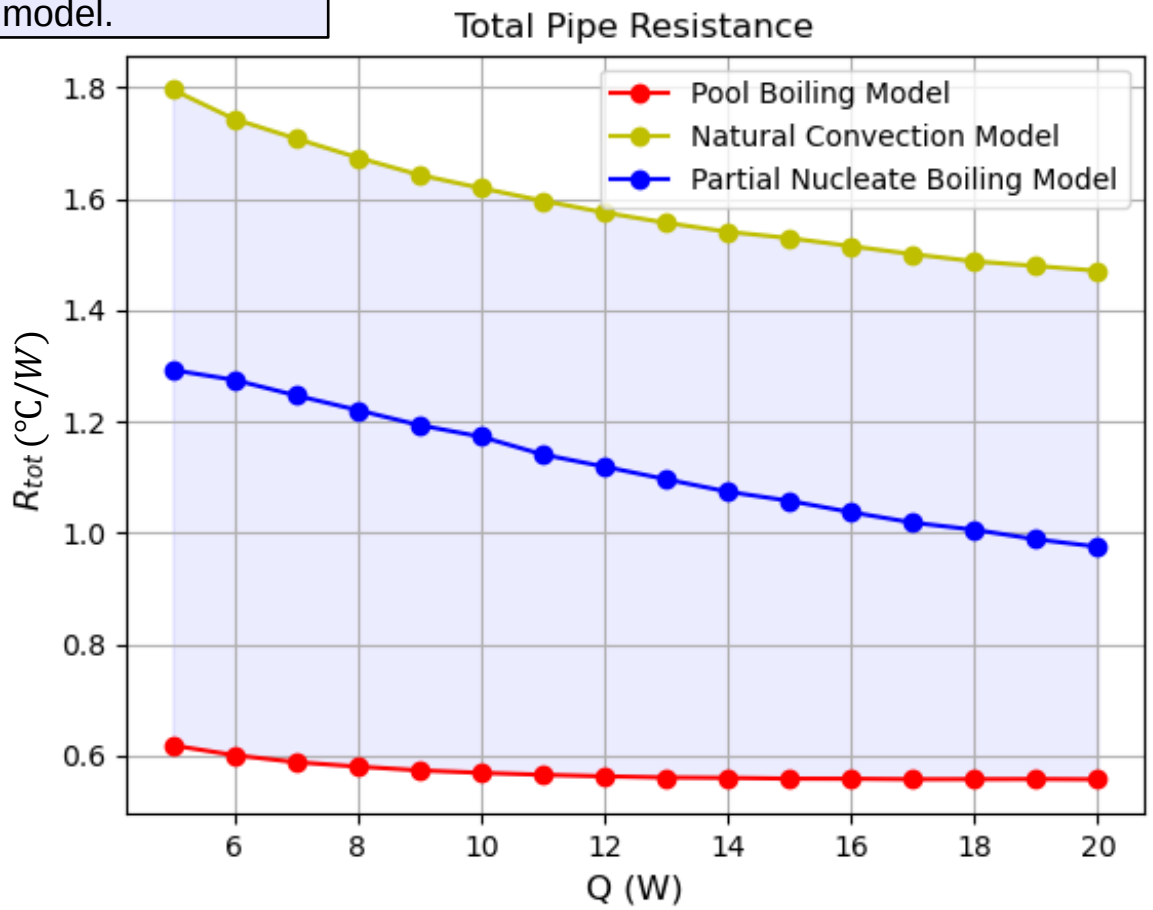

Pipe resistance decreases slightly with higher heat fluxes due to the increased efficiency of boiling and natural convection processes

Experimental Results & Model Comparison – Heat Input Corrected

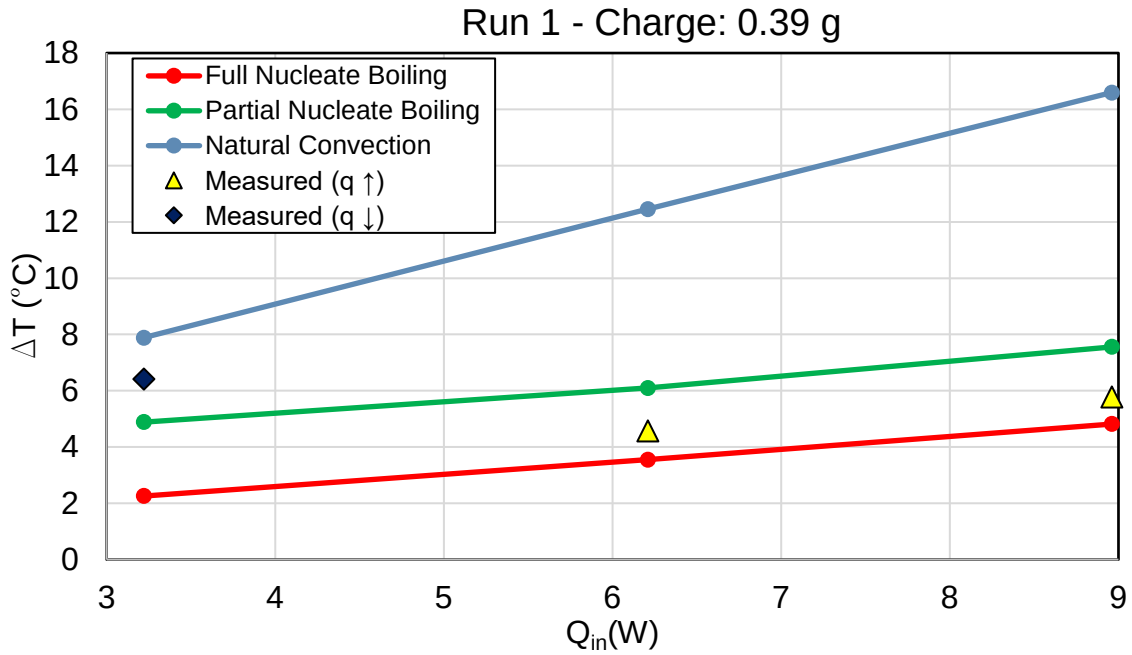

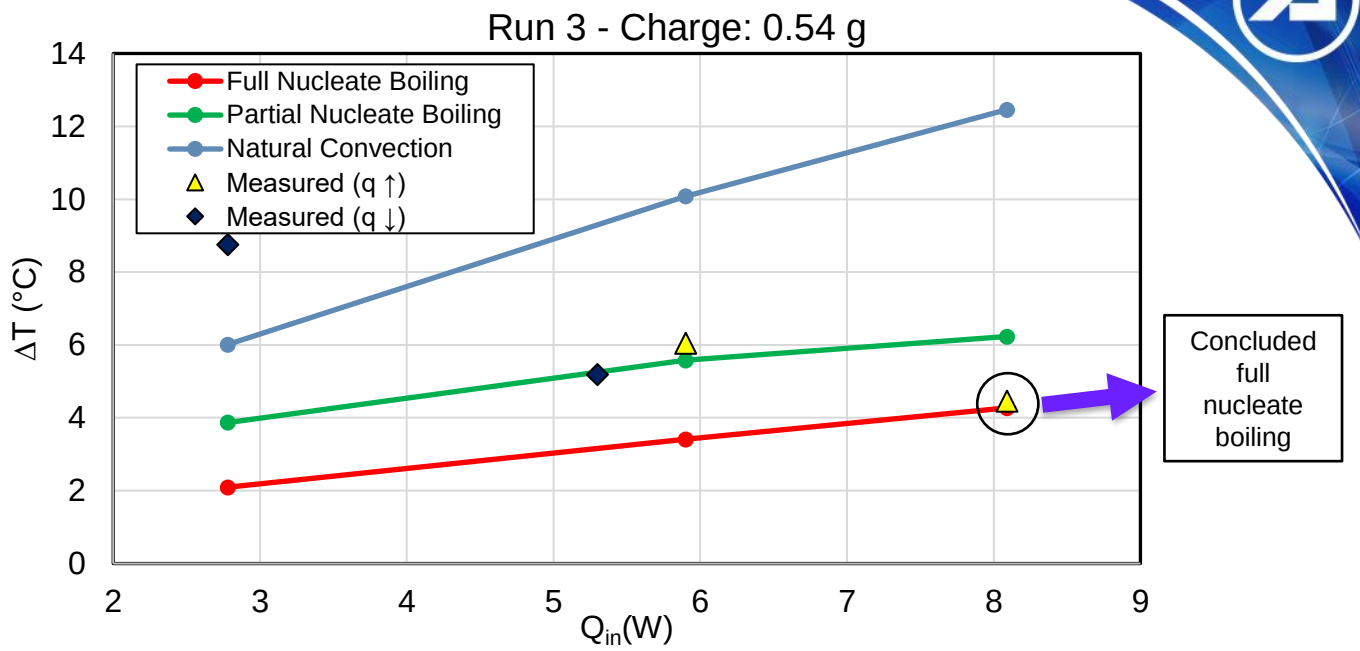

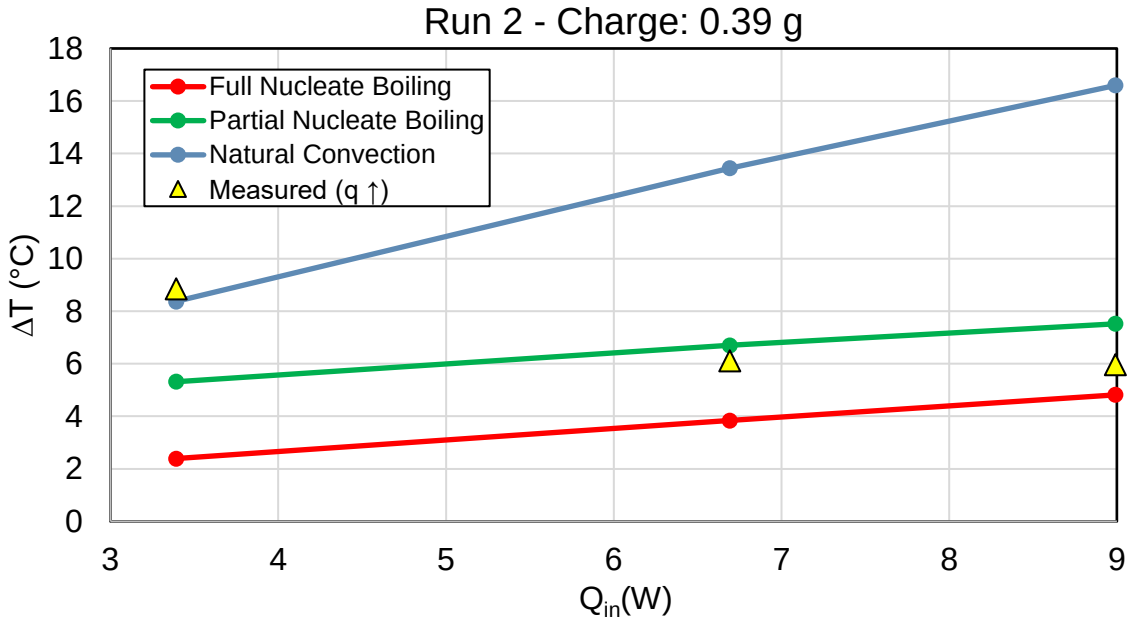

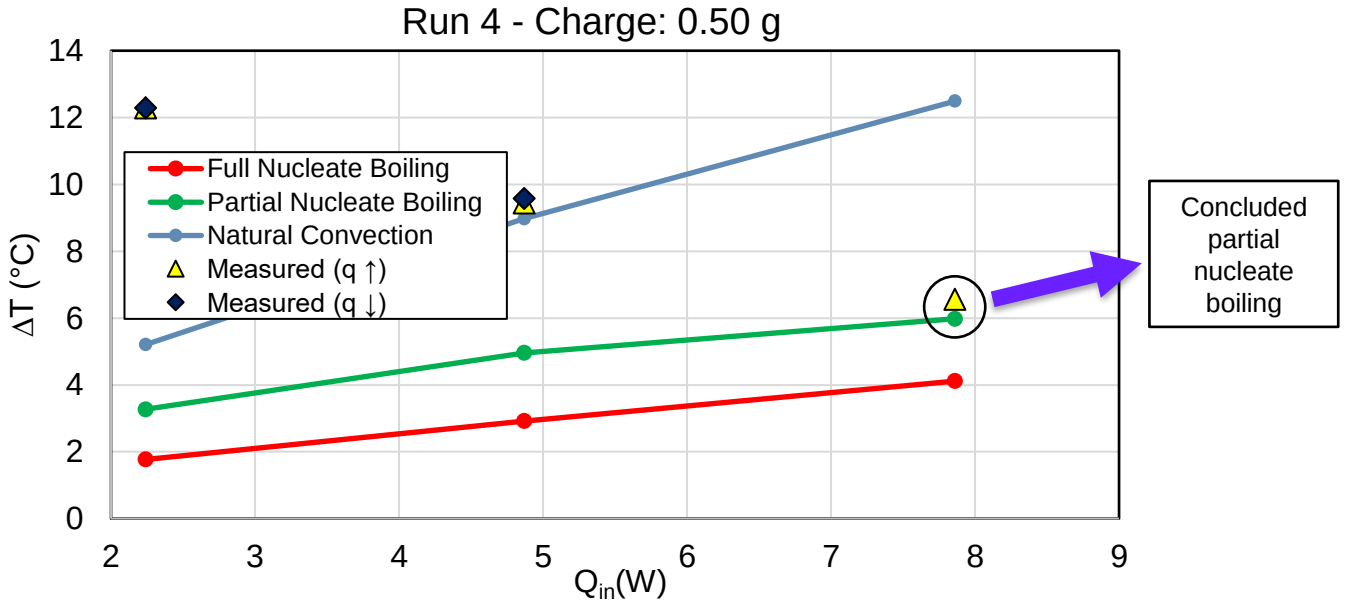

All three evaporator models presented – assessments made about the heat transfer regime for each heat input

Deviation of Results

- Contamination (oxidation, corrosion, oils) can affect boiling characteristics and surface thermal resistance
- Failure to fully purge non-condensable air can degrade condensation performance
  - *Vacuum seal may be degraded due to repeated opening and closing*
- Heat flow losses on exposed evaporator section and through G10 can reduce total heat input
- Filling inaccuracies result in uncertainty of working charge mass
- Uncertainty in thermal conductivity of printed Aluminum

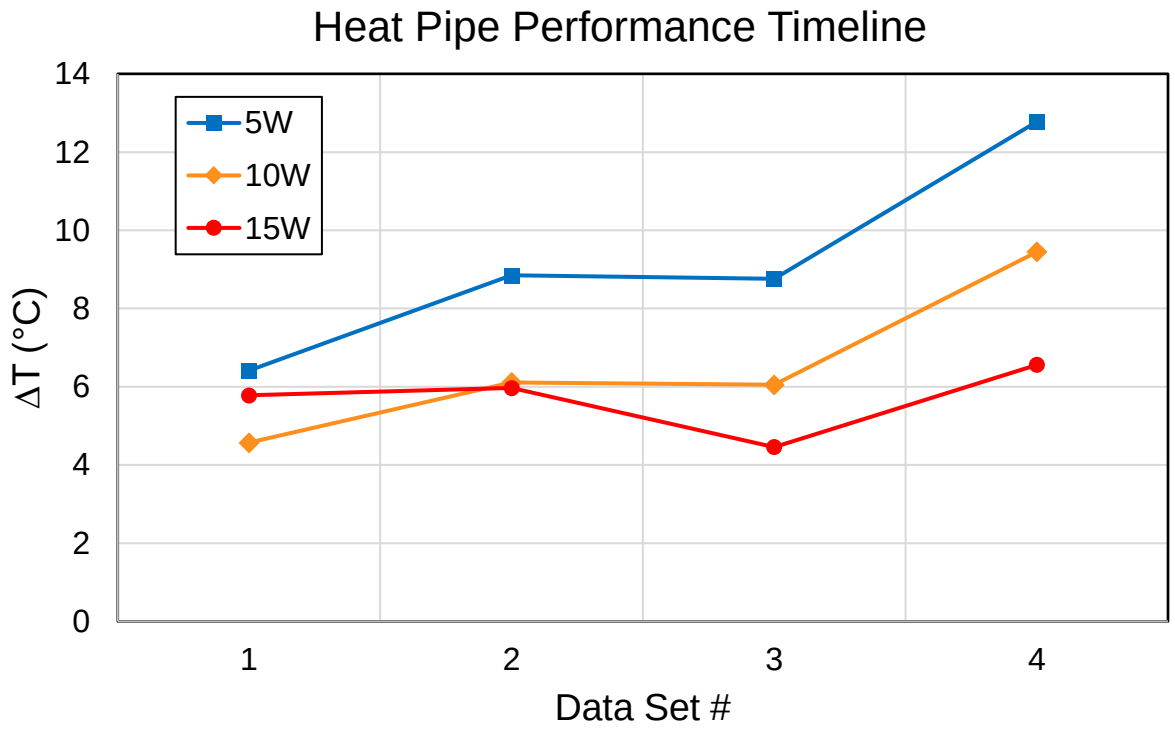

Degradation of heat pipe performance with time indicates changing characteristics within the pipe

Conclusions

- Additively manufactured heat pipes demonstrate successful operation without significant post-process machining required
- Python model matches experimental results within target 25% for 12/15 of cases
  - *25% target corresponds to assessed operating heat transfer mode based on expected boiling behavior and experimental results*
  - *Other 3 of 15 cases may be explained by experimental uncertainties due to temperature measurement, working charge mass, and contamination effects*
  - *Model shows better agreement for early runs, demonstrating that some performance degradation likely occurred over time*
- Future work:
  - *Quantify uncertainty analysis further (sensitivity studies, error propagation, etc.)*
  - *Refine filling and sealing procedure to reduce uncertainty in charge mass and allow for long term (months or years) use*
  - *Use cold plate / pumped fluid loop for condenser heat rejection (allows for maintaining constant condenser heat rejection temperature between runs and eliminates convective loss uncertainty from using a fan)*
  - *Print a test block of known dimensions for thermal conductivity to be measured*
  - *Design an adjustable mount for the heat pipe to be tested at various tilt angles*
  - *Print a larger integrated structure with embedded heat pipes for testing (example: cubesat bus panel)*

Acknowledgments

- David Witkin
- Vinay Goyal
- Mike Benson
- Mike Rosado

Backup Slides

Evaporator Model Flowchart Description

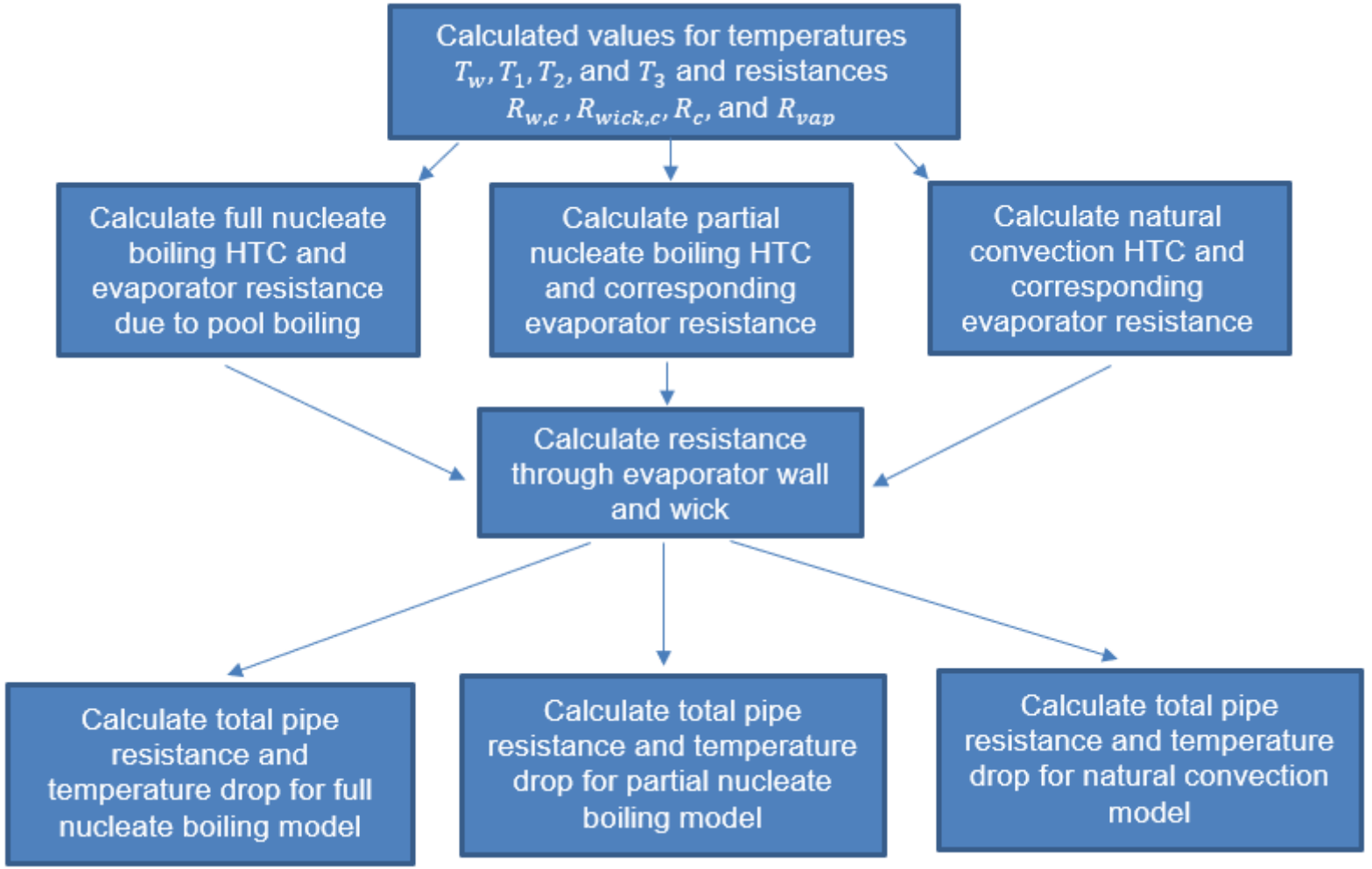

For each heat input, the solution is identical up to the evaporator, and then splits into three solutions corresponding to the different evaporator models

Python Model Overview

Evaporator

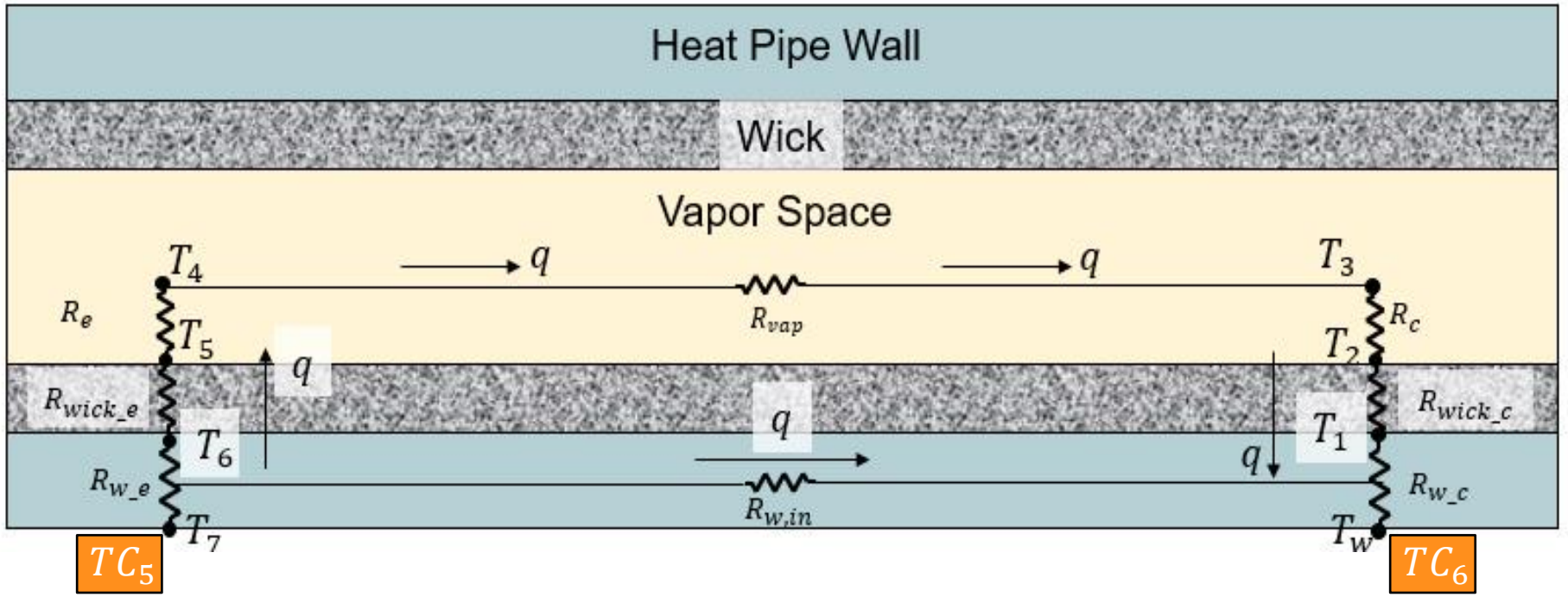

Condenser

- Model inputs: heat pipe cross-section geometry, fluid properties, desired heat input, charge mass, T_w etc.
- Model calculates the resistance between each node, incrementing the temperature to the following node based on the calculated resistance and heat input ($\Delta T = q * R$)
- Condenser resistance (R_c) modeled based on Nusselt film condensation theory
- Evaporator resistance (R_e) corresponds to one of three different evaporator models (natural convection, partial nucleate boiling, full nucleate boiling) to capture delayed onset of boiling which depends on input power
- Model outputs total temperature drop and total pipe resistance for each evaporator model for a specified heat flow range and charge mass

Python Model Sample Outputs

Heat Transfer Coefficients (HTC) & Individual Resistances

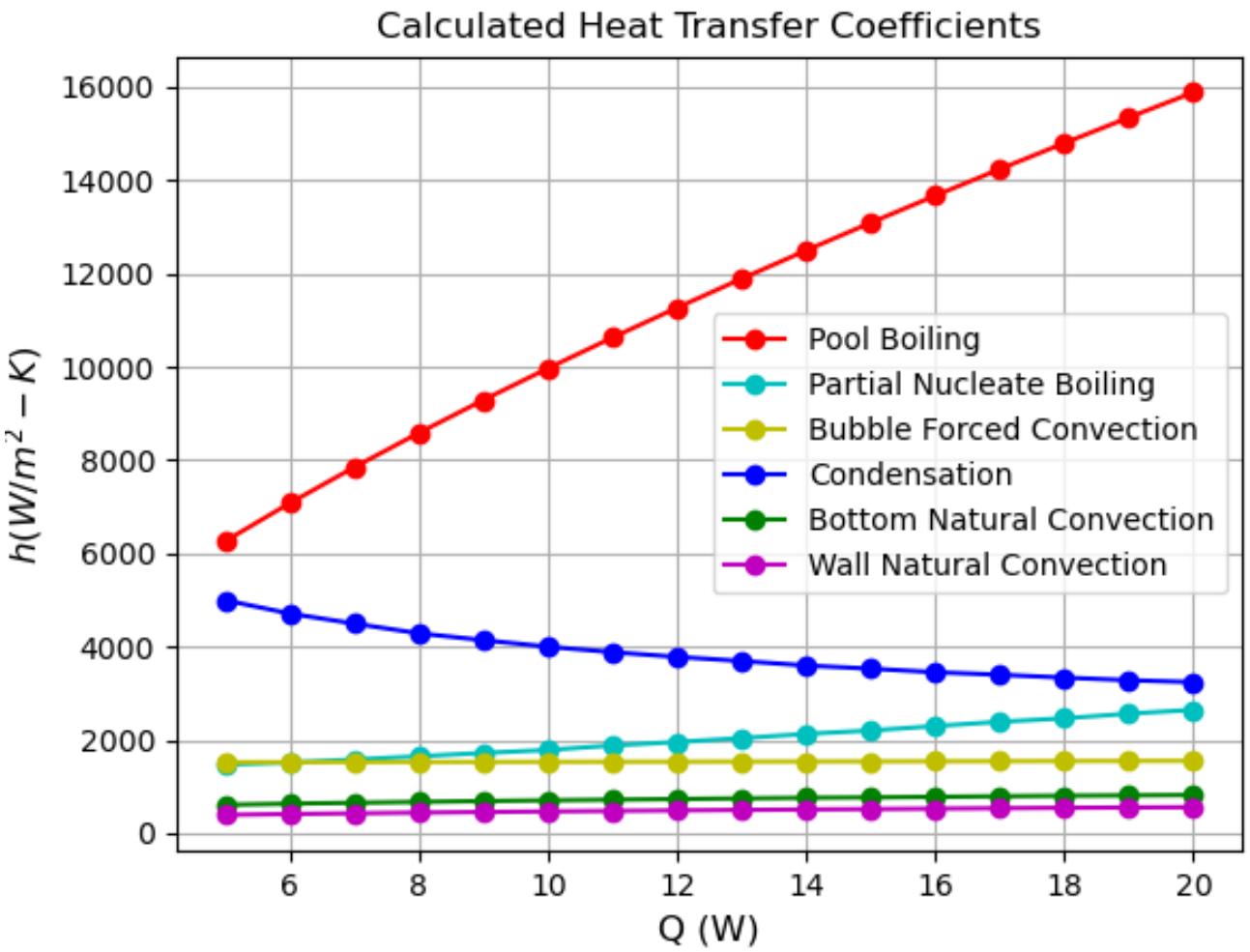

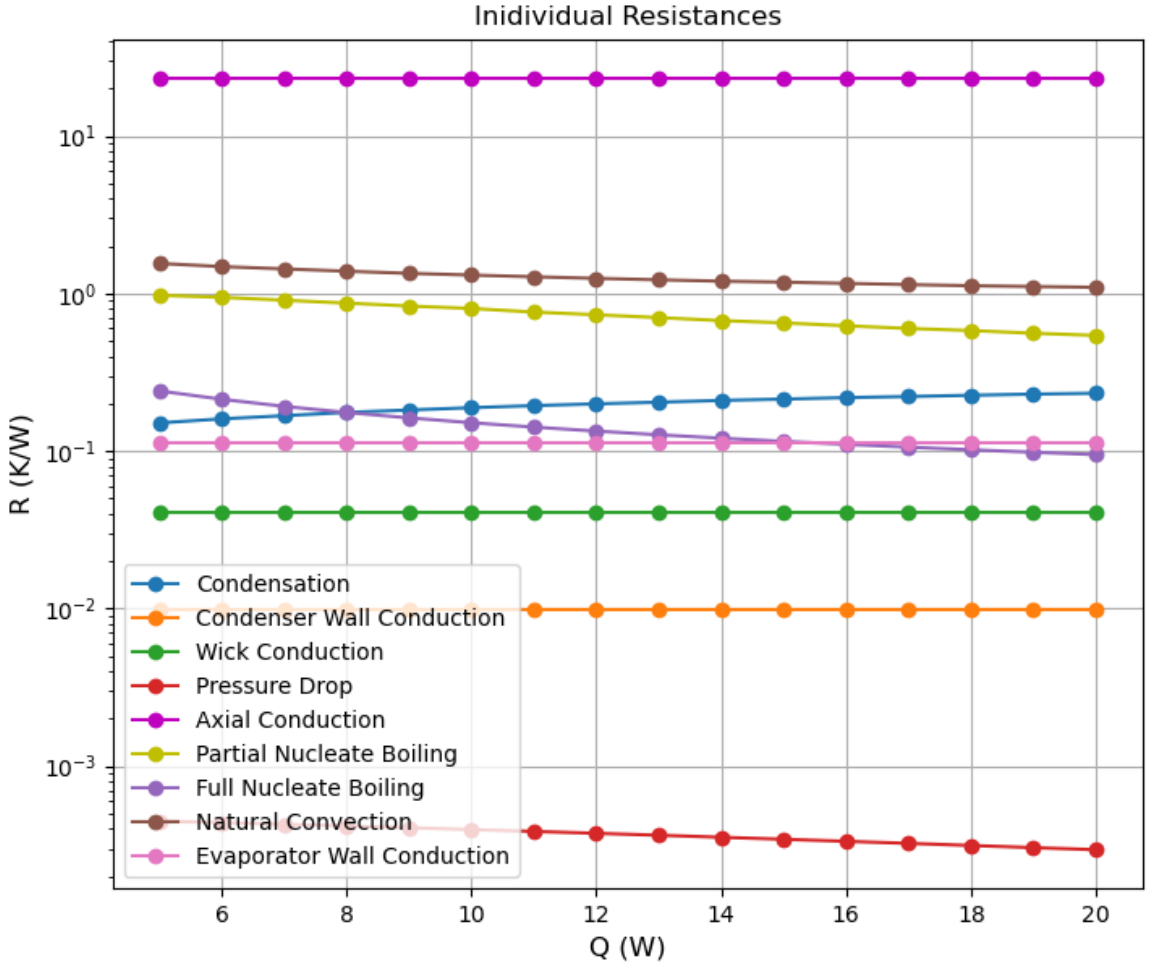

Nucleate pool boiling is the most efficient form of heat transfer within the pipe (high HTC)

Axial conduction is the highest resistance by far, but is in parallel with all others so contribution is small

Test Results Overview – Dry Data Set 1

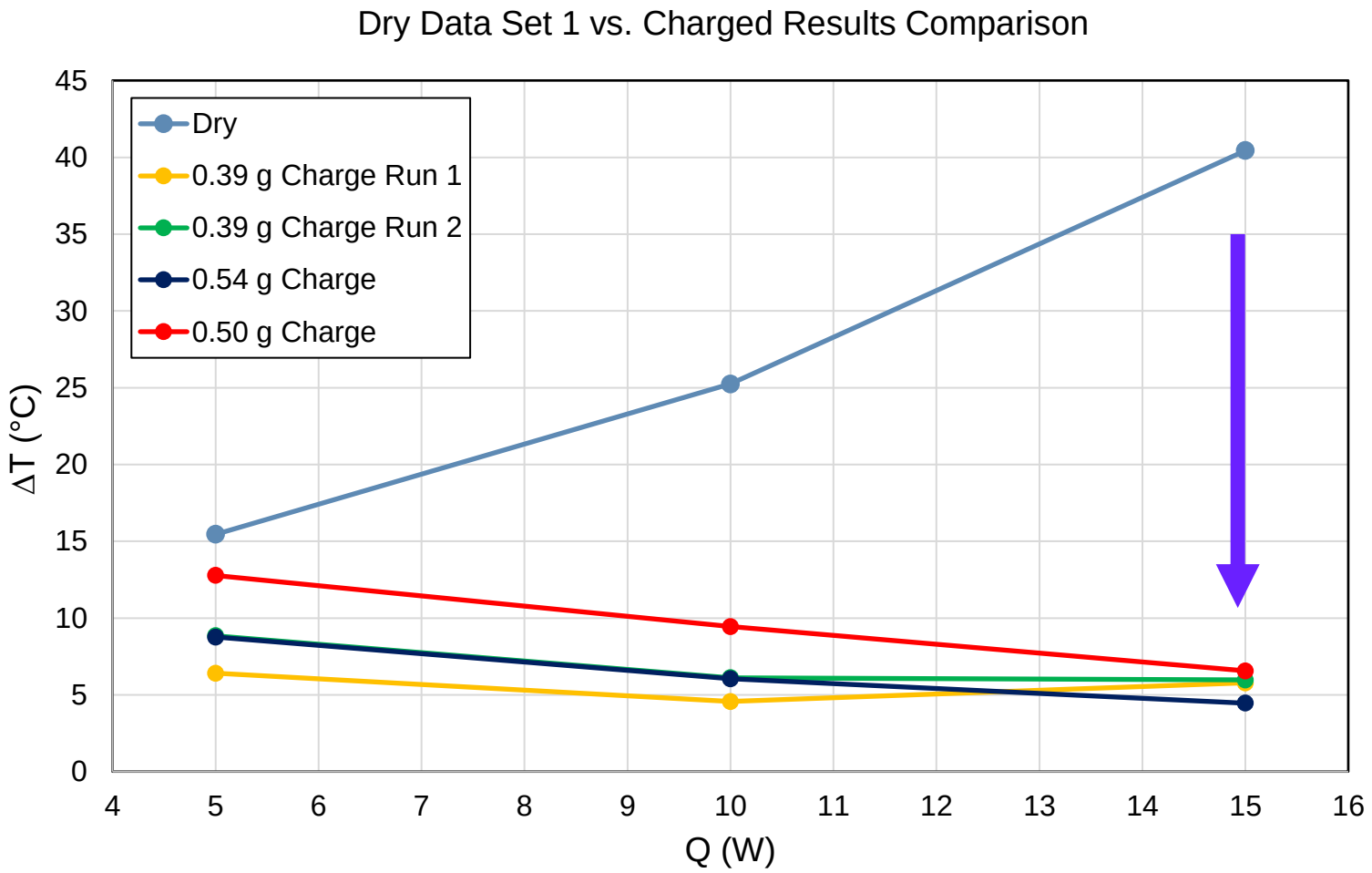

Q (W)	$\Delta T_{filled}/\Delta T_{dry}$
5	0.60
10	0.26
15	0.14

Significant average ΔT reduction seen across all four runs, particularly at higher heat fluxes – heat pipe performance validated

Experimental Results & Model Comparison

Run 1
Charge: 0.39 g

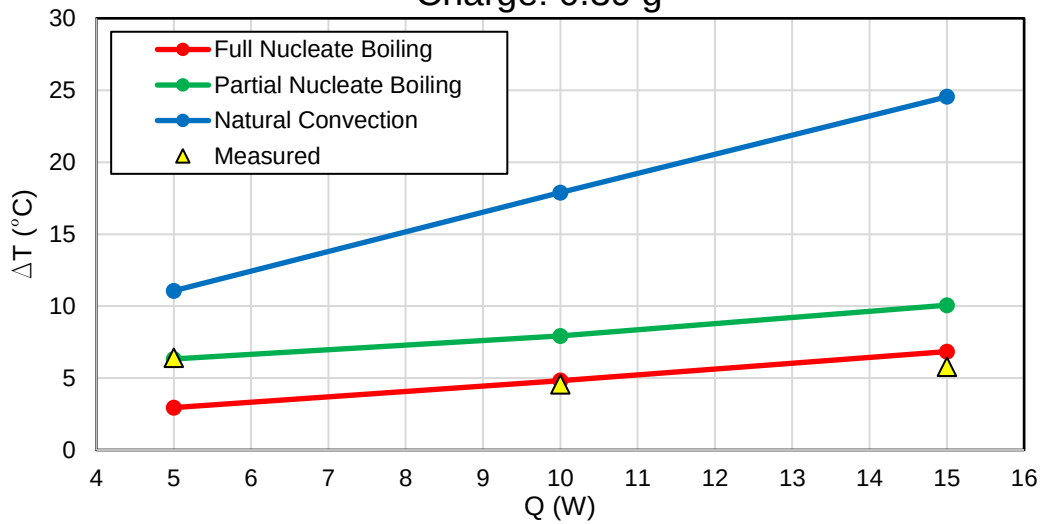

Run 2
Charge: 0.39 g

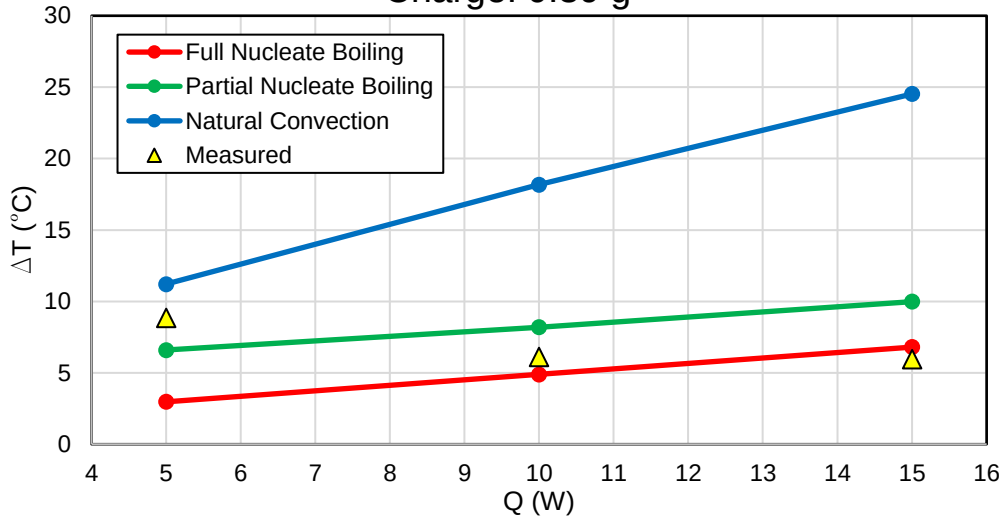

Run 3
Charge: 0.54 g

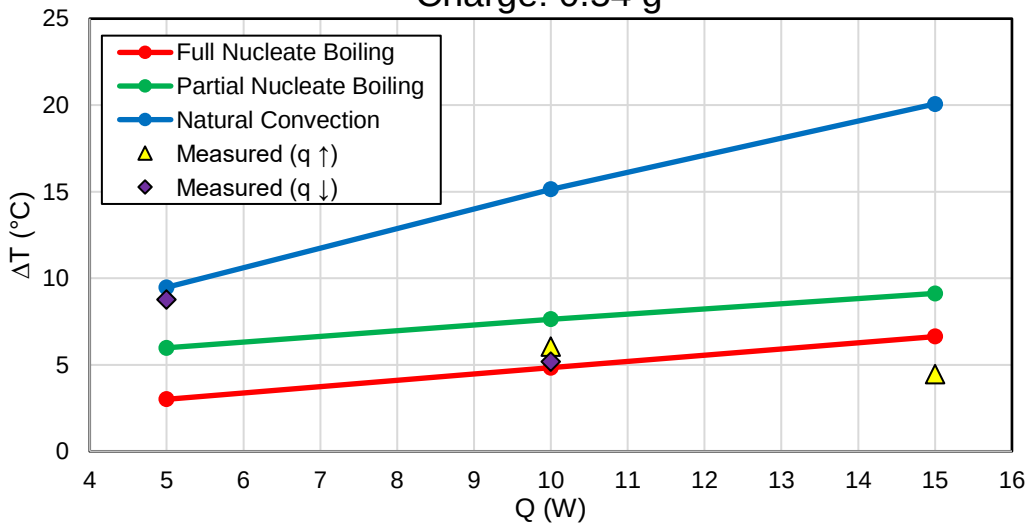

Run 4
Charge: 0.50 g

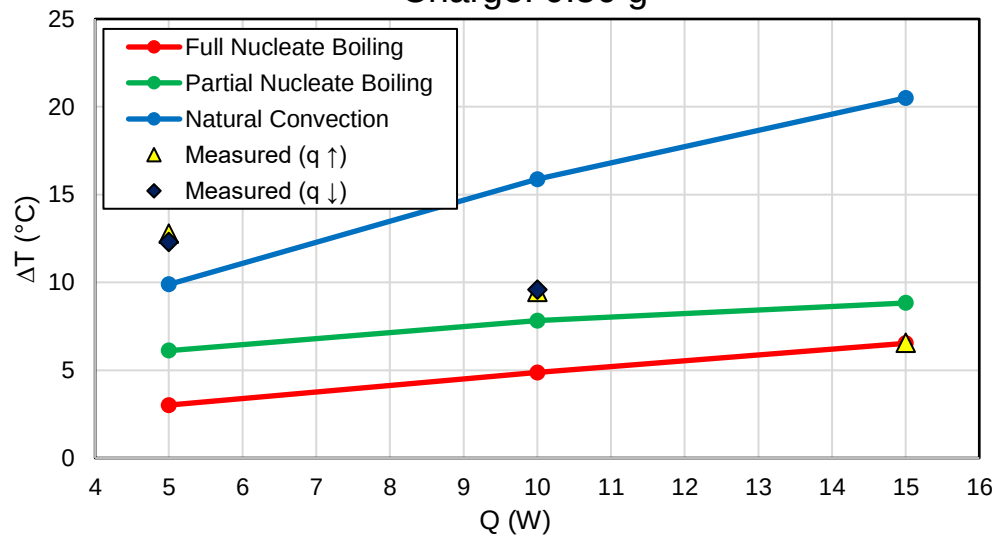

All three evaporator models presented – assessments made about the heat transfer regime for each heat input

Heat Pipe Functionality Verification – Dry Data Set 1

ΔT Comparison – Dry vs. Filled

Q (W)	Dry Measured ΔT (℃)	Run 1 Measured ΔT (℃)	Run 2 Measured ΔT (℃)	Run 3 Measured ΔT (℃)	Run 4 Measured ΔT (℃)	Average ΔT Decrease
5	15.46	6.41	8.85	8.76	12.78	41.23 %
10	25.24	4.57	6.11	6.05	9.45	74.07 %
15	40.44	5.78	5.97	4.46	6.56	85.92 %

Significant ΔT reduction seen – heat pipe performance validated

Heat Pipe Functionality Verification – Dry Data Set 2

ΔT Comparison – Dry vs. Filled

Q (W)	Dry Measured ΔT (℃)	Run 1 Measured ΔT (℃)	Run 2 Measured ΔT (℃)	Run 3 Measured ΔT (℃)	Run 4 Measured ΔT (℃)	Average ΔT Decrease
5	19.27	6.41	8.85	8.76	12.78	41.23 %
10	36.37	4.57	6.11	6.05	9.45	74.07 %
15	51.67	5.78	5.97	4.46	6.56	85.92 %

Significant ΔT reduction seen – heat pipe performance validated

Quantifying Heat Flow Losses – Dry Heat Pipe

SINDA/FLUINT Node Model Verification

Q (W)	Model TC_5 (℃)	Measured TC_5 (℃)	Model ΔT (℃)	Measured ΔT (℃)	h_{fan} $(\frac{W}{m^2-K})$	h_{nat} $(\frac{W}{m^2-K})$	h_{ins} $(\frac{W}{m^2-K})$
5	59.15	57.90	20.60	19.27	18.0	12.0	6.0
10	91.15	91.27	37.70	36.37	18.0	16.0	8.0
15	120.65	121.40	53.50	51.67	18.0	18.0	10.0

- SINDA/FLUINT model used exclusively to quantify heat flow losses
- Fan placed 1.7 in above top of finned heat sink in “pulling” configuration (fan HTC applied to entire heat sink area)
- Relevant geometry measured on experimental setup or SOLIDWORKS model and inputted into Thermal Desktop
- Natural convection HTC applied to evaporator section
- Separate natural convection HTC applied to insulated adiabatic section
- Thermal conductivity of aluminum heat pipe assumed to be $130\frac{W}{m-K}$ (~Al 7075)
- Boundary node for G10 – used temperature from thermocouple recording
  - *G10 thermal conductivity:* $0.288\frac{W}{m-K}$
- Air boundary node fixed at 20 ℃

Quantifying Heat Flow Losses – Results

Dry Heat Pipe

	Convective Losses		Conductive Losses	Heat Input to Heat Pipe	
$Q_{htr}\ (W)$	$Q_{evap-air}\ (W)$	$Q_{ad-air}\ (W)$	$Q_{G10}\ (W)$	$Q_{in}\ (W)$	**% Loss**
5	1.60	0.39	0.67	2.34	53 %
10	3.87	0.80	1.12	4.21	57 %
15	6.16	1.22	1.68	5.96	60 %

- Q_{in} passed into python model to account for heat loss correction
- Dry case provides upper bound for total heat flow losses
- Heat flow losses for filled cases will be lower
  - *Filled heat pipe conductance is much higher than dry heat pipe – in parallel with heat loss conductances results in less heat flow through heat loss branch*

Heater power minus all losses results in actual input power into heat pipe

Quantifying Heat Flow Losses – Filled Heat Pipe Data Set 1

Q (W)	Model TC_5 (℃)	Measured TC_5 (℃)	Model ΔT (℃)	Measured ΔT (℃)	h_{fan} $(\frac{W}{m^2-K})$	h_{nat} $(\frac{W}{m^2-K})$	h_{ins} $(\frac{W}{m^2-K})$	G_{cond} $(\frac{W}{K})$	G_{evap} $(\frac{W}{K})$	G_{vap} $(\frac{W}{K})$
5	59.55	59.02	6.80	6.41	14.0	5.0	5.0	0.25	1.0	0.5
10	87.65	87.12	4.30	4.57	14.0	8.0	5.0	2.0	3.5	0.5
15	96.95	95.83	5.80	5.78	18.0	14.0	7.0	2.0	4.0	0.5
15	107.95	95.83	5.30	5.78	14.0	14.0	7.0	2.0	4.0	0.5

	Convective Losses		Conductive Losses	Heat Input to Heat Pipe	
Q_{htr} (W)	$Q_{evap-air}$ (W)	Q_{ad-air} (W)	Q_{G10} (W)	Q_{in} (W)	% Loss
5	0.67	0.45	0.66	3.22	36 %
10	1.84	0.81	1.14	6.21	38 %
15	3.66	1.07	1.31	8.96	40 %
15	4.19	1.23	1.49	8.09	46 %

- G_{cond} is condenser conductance, G_{evap} is evaporator conductance, and G_{vap} is conductance applied between adiabatic section and vapor node (numerical only)
- $A_c = 0.00132\ m^2; A_e = 0.000664\ m^2$

Quantifying Heat Flow Losses – Filled Heat Pipe Data Set 2

Q (W)	Model TC_5 (℃)	Measured TC_5 (℃)	Model ΔT (℃)	Measured ΔT (℃)	$h_{fan}\ (\frac{W}{m^2-K})$	$h_{nat}\ (\frac{W}{m^2-K})$	$h_{ins}\ (\frac{W}{m^2-K})$	$G_{cond}\ (\frac{W}{K})$	$G_{evap}\ (\frac{W}{K})$	$G_{vap}\ (\frac{W}{K})$
5	55.95	56.39	9.10	8.85	18.0	5.0	5.0	0.125	0.5	0.5
10	79.35	82.61	6.30	6.11	18.0	8.0	5.0	1.25	2.5	0.5
15	96.55	96.44	5.20	5.97	18.0	14.0	7.0	2.5	4.0	0.5

	Convective Losses		Conductive Losses	Heat Input to Heat Pipe	
$Q_{htr}\ (W)$	$Q_{evap-air}\ (W)$	$Q_{ad-air}\ (W)$	$Q_{G10}\ (W)$	$Q_{in}\ (W)$	% Loss
5	0.61	0.40	0.60	3.39	32 %
10	1.61	0.70	1.00	6.69	33 %
15	3.64	1.07	1.30	8.99	40 %

- G_{cond} is condenser conductance, G_{evap} is evaporator conductance, and G_{vap} is conductance applied between adiabatic section and vapor node (numerical only)
- $A_c = 0.00132\ m^2; A_e = 0.000664\ m^2$

Quantifying Heat Flow Losses – Filled Heat Pipe Data Set 3

Q (W)	Model TC_5 (℃)	Measured TC_5 (℃)	Model ΔT (℃)	Measured ΔT (℃)	$h_{fan}\ (\frac{W}{m^2-K})$	$h_{nat}\ (\frac{W}{m^2-K})$	$h_{ins}\ (\frac{W}{m^2-K})$	$G_{cond}\ (\frac{W}{K})$	$G_{evap}\ (\frac{W}{K})$	$G_{vap}\ (\frac{W}{K})$
5	55.85	56.00	7.50	8.76	14.0	10.0	5.0	0.125	0.5	0.5
10	85.15	86.91	4.90	5.19	14.0	10.0	5.0	1.5	3.0	0.5
15	107.95	107.19	5.30	4.46	14.0	14.0	7.0	2.0	4.0	0.5
10	80.05	80.76	6.0	6.05	14.0	14.0	7.0	1.0	2.0	0.5

	Convective Losses		Conductive Losses	Heat Input to Heat Pipe	
$Q_{htr}\ (W)$	$Q_{evap-air}\ (W)$	$Q_{ad-air}\ (W)$	$Q_{G10}\ (W)$	$Q_{in}\ (W)$	% Loss
5	1.22	0.40	0.60	2.78	44 %
10	2.22	0.78	1.10	5.90	41 %
15	4.19	1.23	1.49	8.09	46 %
10	2.86	0.83	1.01	5.30	47 %

- G_{cond} is condenser conductance, G_{evap} is evaporator conductance, and G_{vap} is conductance applied between adiabatic section and vapor node (numerical only)
- $A_c = 0.00132\ m^2; A_e = 0.000664\ m^2$

Quantifying Heat Flow Losses – Filled Heat Pipe Data Set 4

Q (W)	Model TC_5 (℃)	Measured TC_5 (℃)	Model ΔT (℃)	Measured ΔT (℃)	$h_{top}\ (\frac{W}{m^2-K})$	$h_{nat}\ (\frac{W}{m^2-K})$	$h_{ins}\ (\frac{W}{m^2-K})$	$G_{cond}\ (\frac{W}{K})$	$G_{evap}\ (\frac{W}{K})$	$G_{vap}\ (\frac{W}{K})$
5	64.95	60.34	12.90	12.78	10.0	10.0	5.0	0.05	0.10	0.10
10	93.05	89.36	9.80	9.45	11.0	12.0	6.0	0.5	1.5	0.10
15	119.95	116.40	6.60	6.56	12.0	12.0	7.0	1.5	3.0	0.5
10	93.05	90.69	9.80	9.58	11.0	12.0	6.0	0.5	1.5	0.10
5	64.95	61.36	12.90	12.29	10.0	10.0	5.0	0.05	0.10	0.10

	Convective Losses		Conductive Losses	Heat Input to Heat Pipe	
$Q_{htr}\ (W)$	$Q_{evap-air}\ (W)$	$Q_{ad-air}\ (W)$	$Q_{G10}\ (W)$	$Q_{in}\ (W)$	% Loss
5	1.53	0.48	0.75	2.24	55 %
10	2.98	0.92	1.23	4.87	51 %
15	4.07	1.39	1.68	7.86	47 %
10	2.98	0.92	1.23	4.87	51 %
5	1.53	0.48	0.75	2.24	55 %

- G_{cond} is condenser conductance, G_{evap} is evaporator conductance, and G_{vap} is conductance applied between adiabatic section and vapor node (numerical only)
- $A_c = 0.00132\ m^2; A_e = 0.000664\ m^2$
- No fan used in this test – only natural convection on top condenser section

Quantifying Heat Flow Losses – Filled Heat Pipe

SINDA/FLUINT Node Model Verification & Results – Data set 2

Q (W)	Model TC_5 (℃)	Measured TC_5 (℃)	Model ΔT (℃)	Measured ΔT (℃)	h_{fan} $(\frac{W}{m^2-K})$	h_{nat} $(\frac{W}{m^2-K})$	h_{ins} $(\frac{W}{m^2-K})$	G_{cond} $(\frac{W}{K})$	G_{evap} $(\frac{W}{K})$	G_{vap} $(\frac{W}{K})$
5	55.95	56.39	9.10	8.84	18.0	5.0	5.0	0.125	0.5	0.5
5	54.65	56.39	7.40	8.84	15.0	10.0	5.0	0.5	0.125	0.5
5	54.75	56.39	7.70	8.84	15.0	10.0	5.0	0.125	0.5	0.5
10	79.35	82.61	6.30	6.11	18.0	8.0	5.0	1.25	2.5	0.5
10	80.25	82.61	5.50	6.11	15.0	12.0	6.0	1.25	2.5	0.5
15	96.55	96.44	5.20	5.85	18.0	14.0	7.0	2.5	4.0	0.5

	Convective Losses		Conductive Losses	Power Input to Heat Pipe	
Q_{htr} (W)	$Q_{evap-air}$ (W)	Q_{ad-air} (W)	Q_{G10} (W)	Q_{in} (W)	% Loss
5	0.61	0.40	0.60	3.39	32.20 %
5	1.18	0.38	0.58	2.86	42.80 %
5	1.18	0.39	0.58	2.85	43.00 %
10	1.61	0.70	1.00	6.69	33.10 %
10	2.46	0.78	1.02	5.74	42.60 %
15	3.64	1.07	1.30	8.99	40.01 %

- G_{cond} is condenser conductance, G_{evap} is evaporator conductance, and G_{vap} is conductance applied between adiabatic section and vapor node (numerical only)
- $A_c = 0.00132\ m^2; A_e = 0.000664\ m^2$

Deviation of Results: Charge Mass Model Sensitivity Study

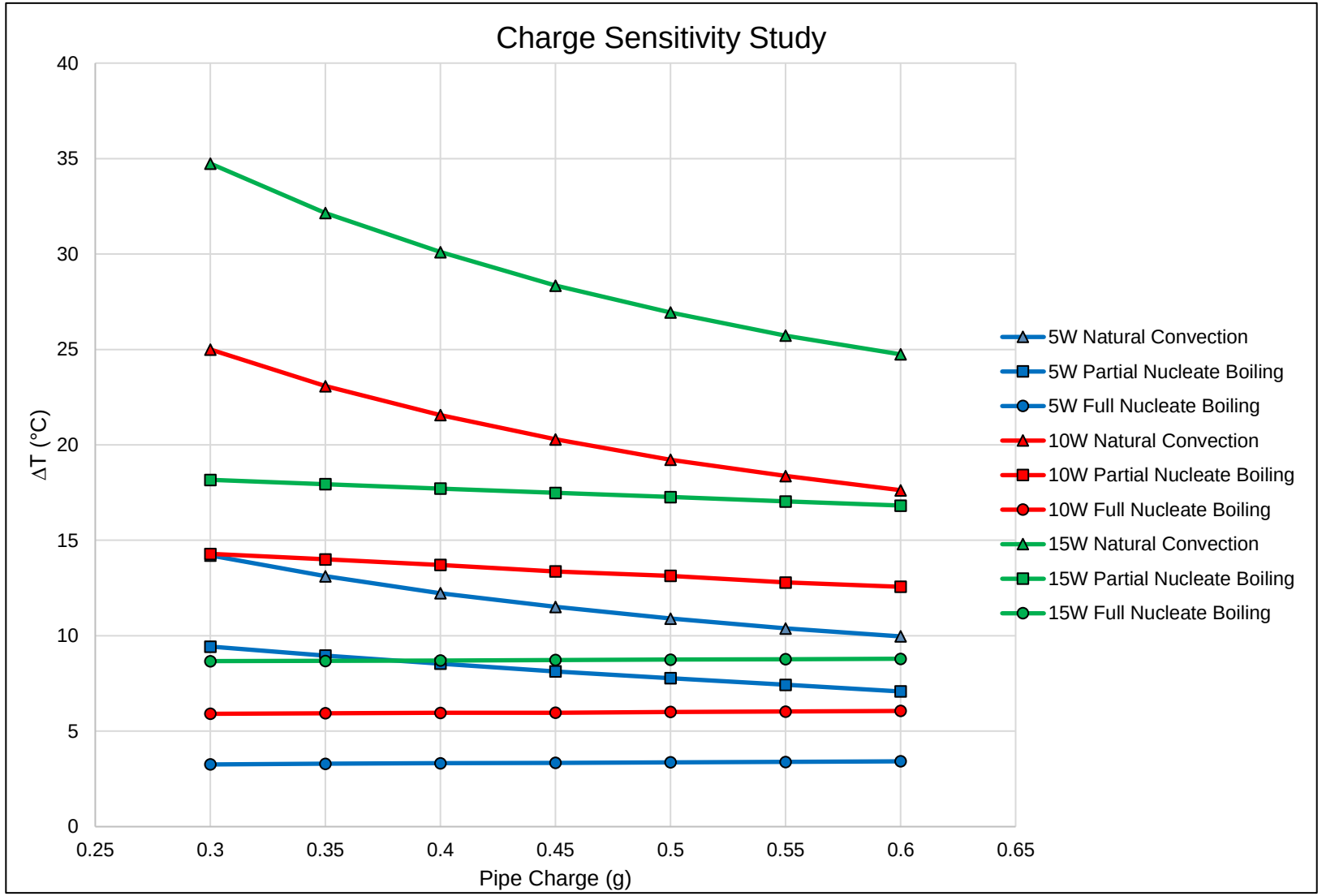

Natural convection model shows very high sensitivity to charge mass (applicable mostly to 5W cases)